Genetic timestamping of plasma cells *in vivo* reveals homeostatic population turnover

Xu AQ[1], Barbosa RR[1], Calado DP[1,2,3*]

1. Immunity and Cancer, The Francis Crick Institute, 1 Midland Road, London NW1 1AT, UK.
2. Peter Gorer Department of Immunobiology, School of Immunology & Microbial Sciences, King's College London, London, UK.
3. Lead contact.

* Corresponding author: Dinis.Calado@crick.ac.uk

Keywords

Jchain, *Blimp1*, *Irf4*, plasma cells, B cells, cre-loxP, homeostasis

Highlights

Jchain expression occurs in most plasma cells across immunoglobulin isotypes

Jchain^{creERT2} mediated genetic manipulation is effective only in plasma cells

Genetic timestamping of plasma cells reveals homeostatic regulation

Abstract

Plasma cells (PC)s are essential for protection from infection, and at the origin of incurable cancers. Current studies do not circumvent limitations of removing PCs from their microenvironment and confound formation and maintenance. This is in part due to the lack of tools to perform specific genetic manipulation *in vivo*. Also, studies of PC population dynamics have mostly relied on the use of nucleotide analog incorporation that does not label quiescent cells, a property of most PCs. Here we characterize in detail a genetic tool (*Jchain*^{creERT2}) that permits first-ever specific genetic manipulation in PC *in vivo*, across immunoglobulin isotypes. Using this tool we found that PC numbers remained constant over-time and that PC decay was compensated by the emergence of new cells, supporting an homeostatic turnover of the population. The *Jchain*^{creERT2} genetic tool paves the way for in-depth mechanistic understanding of PC biology and pathology *in vivo*, in their microenvironment.

57 **Introduction**

58 Antibodies produced by plasma cells (PCs) are crucial for immune protection against infection and for
59 vaccination success (Nutt et al., 2015). Upon activation B cells terminally differentiate into PCs, a
60 process initiated by the downregulation of the B cell transcription factor PAX5 (Kallies et al., 2007).
61 This event allows the expression of multiple factors normally repressed by PAX5, including *Xbp1*and
62 *Jchain* (Castro and Flajnik, 2014; Nutt et al., 2015; Rinkenberger et al., 1996; Shaffer et al., 2004).
63 PAX5 downregulation is also followed by the expression of the transcription factors IRF4 and BLIMP1
64 that play essential roles in the establishment of the PC program (Kallies et al., 2007; Klein et al., 2006;
65 Shapiro-Shelef et al., 2003). Beyond physiology, multiple cancers have a PC as cell of origin, including
66 multiple myeloma, the second most frequent hematological malignancy overall, for which a cure
67 remains to be found (Palumbo and Anderson, 2011). As consequence, the study of gene function in PC
68 biology and pathology is a subject of intense investigation.

69

70 However, at least in part because of technical limitations most PC studies make use of *in vitro* and cell
71 transfer systems that remove PCs from their microenvironment. Currently, genetic manipulation of PCs
72 is not specific and targets other cell populations such as B cells, confounding PC formation and
73 maintenance. Also, studies on the global turnover of the PC population are lacking, as investigation of
74 the regulation of PC maintenance has mostly relied on the use of nucleotide analogs that do not track
75 the vast majority of PCs due to their quiescent nature.

76

77 We found that amongst well-known PC associated genes, *Jchain* (*Igj*) had the highest level and most
78 specific expression in PC populations. JCHAIN is a small polypeptide required to multimerize IgM and
79 IgA, and necessary for the transport of these Ig classes across the mucosal epithelium in a poly-Ig
80 receptor mediated process (Brandtzaeg and Prydz, 1984; Castro and Flajnik, 2014; Max and Korsmeyer,
81 1985). Here we characterized in detail a GFP-tagged creERT2 allele at the *Jchain* endogenous locus:
82 $Igj^{creERT2}$, hereafter termed $Jchain^{creERT2}$. We found at the single cell level that *Jchain* expression
83 occurred in PCs across immunoglobulin isotypes, including IgG1. Using the $Jchain^{creERT2}$ allele we
84 performed the first-ever highly specific cre-loxP genetic manipulation in PCs residing in their natural

microenvironment *in vivo*. Using this system, that allows inclusive genetic timestamping of plasma cells, independent of their cell cycle status, we uncovered that the numbers of PCs in the spleen and bone marrow remained constant over-time and that PC decay was compensated by the emergence of new PCs. These data suggest that the turnover of the plasma cell population is homeostatically regulated. The *Jchain*^{creERT2} is thus a validated plasma cell specific genetic tool that paves the way for in-depth mechanistic understanding of PC biology and pathology *in vivo*, in their microenvironment.

113 **Results**

114 ***Jchain* transcripts are highly enriched in plasma cells**

115 B-to-PC differentiation is a process that involves a complex network of factors (**Fig. 1A**; (Nutt et al.,
116 2015)). We investigated the level and specificity of the expression of genes associated with PCs (*Xbp1*,
117 *Jchain*, *Scd1*, *Irf4*, and *Prdm1*) through the analysis of a publicly available RNA sequencing dataset for
118 immune cell populations (ImmGen, (Heng et al., 2008)). We first determined the cell populations with
119 the highest transcript level for each factor. *Xbp1* and *Irf4* were primarily expressed in PCs, however the
120 expression in bone marrow PCs (B_PC_BM) was less than 2-fold greater than that of non-PC
121 populations (**Fig. 1B**). The expression of *Sdc1* and *Prdm1* was not specific to PCs (**Fig. 1C**). Notably,
122 peritoneal cavity macrophages (MF_226+II+480lo_PC) expressed more *Sdc1* than bone marrow PCs
123 (B_PC_BM), and a subset of FOXP3^{+} T cells (Treg_4_FP3+_Nrplo_Co) expressed higher levels of
124 *Prdm1* than that observed in splenic plasmablasts (B_PB_Sp) and bone marrow PCs (B_PC_BM; **Fig.**
125 **1C**). In contrast, *Jchain* had the highest level of transcript expression in PCs compared to non-PCs and
126 was the most PC specific amongst all factors, with a 40-fold enrichment over germinal center (GC) B
127 cells (B_GC_CB_Sp; **Fig. 1D**). We concluded that the *Jchain* locus was a suitable candidate for the
128 generation of PC specific genetic tools.

129

130 ***Jchain* is expressed in a small fraction of GC B cells and in most plasma cells**

131 We searched alleles produced by the EUCOMMTools consortium and identified a genetically
132 engineered *Jchain* allele produced by the Wellcome Trust Sanger Institute: MGI:5633773, hereafter
133 termed *Jchain*$^{\text{creERT2}}$. The genetically engineered *Jchain* allele contained an *FRT* site between exons 1
134 and 2 followed by an engrailed 2 splice acceptor sequence and an *EGFP.2A.cre*^{ERT2} expression cassette
135 (**Fig. 2A**). In this design the expression of the EGFP (GFP) and of creERT2 is linked by a self-cleaving
136 2A peptide under the transcriptional control of the *Jchain* promoter (**Fig. 2A**). To determine cells with
137 GFP expression we initially analyzed the spleen from mice heterozygous for the *Jchain*$^{\text{creERT2}}$ allele that
138 had been immunized with sheep red blood cells (SRBC) 12 days earlier **(Fig. 2B)**. B220 is expressed
139 on the surface of B cells and downregulated during PC differentiation (Pracht et al., 2017). We therefore
140 defined three cell populations based on the levels of GFP fluorescence and B220 surface expression:

141 GFP^{low}B220^{high}, GFP^{int}B220^{int}, GFP^{high}B220^{low}, and a population negative for both markers
142 (GFP^{neg}B220^{neg}; **Fig. 2C**). We next determined the fraction of cells within these populations That
143 expressed surface CD138, a commonly used marker to define PCs by flow-cytometry (Pracht et al.,
144 2017). The GFP^{neg}B220^{neg} population did not contain CD138^{+} cells, however, the fraction of CD138^{+}
145 cells increased in the remaining populations in agreement with the reduction of B220 expression during
146 PC differentiation, and the GFP^{int}B220^{int} and GFP^{high}B220^{low} populations were mostly composed of
147 CD138^{+} cells (**Fig. 2D** and **E**). Identical results were found when defining PCs using in addition surface
148 expression of CXCR4. a chemokine receptor that facilitates homing of PCs to the bone marrow (**Fig.
149 2D** and **E**; (Hargreaves et al., 2001)). We further investigated the cellular composition of the
150 GFP^{low}B220^{high} population that contained the fewest CD138^{+} cells (1 to 20%; **Fig. 2E**). We found that
151 virtually all CD138^{neg} cells within the GFP^{low}B220^{high} population expressed the B cell marker CD19
152 (**Fig. 2F**). Also, and in agreement with *Jchain* gene expression analysis (**Fig. 1D**), these cells were
153 mostly germinal center (GC) B cells (CD38^{low}FAS^{high}; **Fig. 2F** and **G**). We further performed analyses
154 in the spleen and bone marrow of 12-day SRBC immunized mice heterozygous for the *Jchain*^{creERT2}
155 allele in which precursors and mature B cells, and non-B cell populations were first defined using
156 surface markers and the fraction of GFP expressing cells within those populations determined (**Fig. S1**).
157 We found that most PCs (CD138^{+}CXCR4^{+}, 60 to 90%) in the spleen and bone marrow expressed GFP
158 (**Fig. S1**). We also observed that a minor fraction of B1b cells (0 to 6%) in the spleen expressed GFP,
159 possibly in agreement with the knowledge that B1b cells are prone to differentiate into PCs and are a
160 source of IgM antibodies during T cell independent responses (Alugupalli et al., 2004). Collectively
161 these data confirmed at the single cell level the gene expression analysis using bulk populations (**Fig.
162 1D**) and demonstrated that *Jchain* expression is highly enriched in PCs.
163

164 ***Jchain* expression correlates with that of IRF4 and BLIMP1**

165 IRF4 and BLIMP1 transcription factors play an essential role in PC differentiation (Kallies et al., 2007;
166 Klein et al., 2006; Shapiro-Shelef et al., 2003). We analyzed the spleen of 12-day SRBC immunized
167 mice heterozygous for the *Jchain*^{creERT2} allele and determined the expression pattern of IRF4 and
168 BLIMP1 in the populations defined by varied GFP and B220 expression (**Fig. 2C**, **3A** and **B**). The

169 GFP^{neg}B220^{neg} population was virtually devoid of cells with BLIMP1 and IRF4 expression (**Fig. 3C**).
170 In contrast the GFP^{low}B220^{high} cell population contained ~7% (median) of BLIMP1^{+}IRF4^{+} cells (**Fig.**
171 **3D** and **E**). These *in vivo* data suggested that *Jchain* expression precedes that of IRF4 and BLIMP1,
172 something previously suggested from *in vitro* cultures of *Blimp1* deficient B cells (Kallies et al., 2007).
173 Still, *Jchain* expression strongly correlated with that of IRF4 and BLIMP1 given that the vast majority
174 of cells within the GFP^{int}B220^{int} and GFP^{high}B220^{low} populations were BLIMP1^{+}IRF4^{+} (**Fig. 3D** and **E**).
175 Overall we identified an *in vivo* population of cells in which *Jchain* expression precedes that of IRF4
176 and BLIMP1, possibly representing PC precursors. As PC differentiation ensues, *Jchain* expression
177 correlates highly with the expression of the transcription factors BLIMP1 and IRF4 that are critical for
178 the establishment of the PC program.
179

180 ***Jchain*^{creERT2} mediated genetic manipulation is effective only in plasma cells**

181 We next sought to determine whether the *Jchain*^{creERT2} allele could be used to perform genetic
182 manipulation of PCs. For that we generated compound mutant mice carrying the *Jchain*^{creERT2} allele and
183 a Rosa 26 allele in which RFP expression is conditional to cre-mediated recombination of a loxP-STOP-
184 loxP cassette (*R26*^{lslRFP}; (Luche et al., 2007)). In the *Jchain*^{creERT2} allele, cre is fused to an estrogen
185 binding domain (ERT2) that sequesters cre in the cytoplasm through the binding to HSP90 (Feil et al.,
186 2009) . Addition of tamoxifen displaces the creERT2-HSP90 complex allowing effective nuclear import
187 of creERT2 and its access to loxP flanked DNA sequences (Feil et al., 2009). We first performed an *in*
188 *vitro* experiment using a classical plasmablast (B220^{low}CD138^{+}) differentiation assay in which B cells
189 purified from mice carrying the *Jchain*^{creERT2} and *R26*^{lslRFP} alleles were cultured with LPS in the presence
190 or absence of 4-OH tamoxifen (Andersson et al., 1972). GFP expression was highly enriched in
191 plasmablasts compared to B cells and RFP expression was only observed upon addition of 4-OH
192 tamoxifen to the cell culture, and that occurred virtually only in plasmablasts (**Fig. S2**). This data
193 suggested that creERT2 was specifically expressed by plasmablasts and effectively retained in the
194 cytoplasm in the absence of 4-OH tamoxifen. Similar observations were made in mice carrying the
195 *Jchain*^{creERT2} and *R26*^{lslRFP} alleles *in vivo*. In the absence of tamoxifen administration RFP expressing
196 cells were not detected, confirming the *in vitro* results and supporting that the *Jchain*^{creERT2} allele was

197 not "leaky" in the control of cre activity (**Fig. S1B**, **C** and **E**). We next immunized mice carrying
198 *Jchain*^{creERT2} and *R26*^{lslRFP} alleles and administered tamoxifen on days 7, 8, 9 and 10 followed by
199 analysis of spleen and bone marrow at day 12 (**Fig. 4A**). Analyses of the populations defined by varied
200 GFP and B220 surface expression (**Fig. 2** and **4B**) revealed that a small fraction of GFP^{low}B220^{high} cells
201 were positive for RFP in the spleen (median ~2%) and in the bone marrow (median ~1.2%; **Fig. 4C**).
202 In contrast, cre mediated recombination and as consequence RFP expression occurred in ~37% and
203 ~31% of GFP^{int}B220^{int} in the spleen and bone marrow, respectively, whereas the vast majority of cells
204 within the GFP^{high}B220^{low} population had undergone cre mediated recombination and were RFP
205 positive (~76% in the spleen, and ~88% in the bone marrow, median; **Fig. 4C** and **D**). These data
206 showed that *Jchain*^{creERT2} mediated cre-recombination was only effective in PC populations validating
207 it as a tool to specifically perform genetic manipulation of PCs.
208
209 **Genetic manipulation using *Jchain*^{creERT2} occurs across immunoglobulin isotypes**
210 IgG1 does not multimerize, and due to differences in its secretory tail to that of IgA and IgM, JCHAIN
211 does not associate with IgG1 (Johansen et al., 2000). Currently it is suggested that *Jchain* expression
212 occurs in all PCs regardless of isotype (Castro and Flajnik, 2014; Johansen et al., 2000; Mather et al.,
213 1981). However, this has not been demonstrated at the single cell level. We performed experiments that
214 investigated whether *Jchain*^{creERT2} allele GFP expression (as proxy for *Jchain*), and cre-mediated loxP
215 recombination occurred in PCs across immunoglobulin isotypes. For that we analyzed the spleen,
216 mesenteric lymph nodes (mLN), peyer's patches and bone marrow of younger (15 weeks) and older (30
217 weeks) mice carrying the *Jchain*^{creERT2} and *R26*^{lslRFP} alleles. These mice were immunized with SRBC
218 and administered with tamoxifen on days 7, 8, 9 and 10 followed by analysis at day 12 (**Fig. 5A**). We
219 first analyzed total PCs (B220^{low}CD138^{+}), and within these cells those that expressed GFP (RFP^{+} and
220 RFP^{neg}, i.e. *Jchain*$^{+}$) and GFP^{+}RFP^{+} cells (i.e. *Jchain*$^{+}$ and cre recombined) to determine the proportions
221 of IgA, IgM and IgG1 expressing cells using intracellular stain (**Fig. 5B-D**). Overall we found only
222 small differences. Analysis of spleens of 15-week-old mice revealed a slight increase in the percentage
223 of IgA^{+} cells within the GFP^{+}RFP^{+} PCs only when compared to total PCs (**Fig. 5E**). A similar trend
224 was observed when analyzing the peyer's patches of 15-week-old mice (**Fig. 5E**). However, in these

225 mice we did not observe differences in the proportion of IgA of other analyzed tissues, nor for IgM and
226 IgG1 in any of the tissues analyzed (**Fig. 5E**). 30-week-old mice showed a slight increase in the
227 percentage of splenic IgM^+ cells within the GFP^+RFP^+ PCs only when compared to total PCs, and for
228 IgA^+ in the mesenteric lymph node (mLN; **Fig. 5F**). No significant difference were observed in 30-
229 week-old mice for the proportion of IgM or IgA in any of the other analyzed tissues, and in none of the
230 analyzed tissues for IgG1 (**Fig. 5F**). Taken together, these data suggested that *Jchain* expression is not
231 overly represented in IgA or IgM expressing PCs compared to $IgG1^+$ PCs. We conclude that
232 *Jchain*^{creERT2} mediated cre-loxP recombination occurs across immunoglobulin isotypes and thus for
233 genetic manipulation also of PCs expressing IgG1.
234
235 **Inclusive analysis of plasma cell dynamics reveals homeostatic population turnover**
236 Understanding of the PC population turnover is lacking. Multiple investigations have been performed
237 to determine the PC life-span using primarily nucleotide analog DNA incorporation. These studies have
238 provided fundamental insights on PC maintenance and currently it is accepted that a fraction of PCs in
239 the mouse survives for periods longer than 3 months (Ho et al., 1986; Lemke et al., 2016; Manz et al.,
240 1998; Manz et al., 1997; Slifka et al., 1998). However, given the quiescent nature of PCs and that
241 nucleotide analog methodology requires cell division, it is not appropriate to study global population
242 turnover. We investigated the suitability of the *Jchain*^{creERT2} allele to determine the turnover of the PC
243 population in the spleen and bone marrow. We immunized mice carrying the *Jchain*^{creERT2} and *R26*^{lslRFP}
244 alleles at two time-points spaced by a period of 21 days (**Fig. 6A**, (Calado et al., 2010)). Thirty days
245 after the secondary immunization (day 51) we administered tamoxifen for 5 consecutive days to
246 genetically label PCs (**Fig. 6A**). Next we determined the absolute cell number of total PCs, of GFP^+
247 cells (RFP^+ and RFP^{neg}, i.e. *Jchain*$^+$), GFP^+RFP^+ cells (i.e. *Jchain*$^+$ cre recombined), and GFP^+RFP^{neg}
248 cells (i.e. *Jchain*$^+$ not cre recombined). We found that over a period of 5 months the cell number of total
249 and GFP^+ PCs remained constant over time (**Fig. 6B** and **C**). In contrast the cell number of GFP^+RFP^+
250 cells decayed (**Fig. 6B** and **C**) in both spleen ($t_{1/2}$ ~31.63d) and bone marrow ($t_{1/2}$ ~251.93d; **Fig. 6D** and
251 **E**). These results agree with the knowledge that the half-life of PCs differs between spleen and the bone
252 marrow (Sze et al., 2000). Notably, analysis of the GFP^+RFP^{neg} cell numbers revealed that the

253 emergence of these cells paralleled that observed for the decay of GFP^+RFP^+ cells (**Fig. 6B** and **C**) both
254 in spleen ($t_{1/2}$ ~20.20d) and bone marrow ($t_{1/2}$ ~190.19d; **Fig. 6D** and **E**). These data indicate that the
255 turnover of the *Jchain*$^+$ PC population, representing 70 to 90% of all PCs in spleen and bone marrow
256 (**Fig S2B** and **C**), is homeostatically regulated.
257
258
259
260
261
262
263
264
265
266
267
268
269
270
271
272
273
274
275
276
277
278
279
280

281 **Discussion**

282 Plasma cells (PC)s are an essential component of the adaptive immune system. However, compared to
283 other B cell lineage populations the molecular analysis of PC gene function *in vivo* has lagged behind.
284 One underlying cause is the lack of tools for specific genetic manipulation in PCs, something available
285 for B cells since 1997, more than 20 years ago (Rickert et al., 1997), and more recently for B cells at
286 multiple stages of development (Boross et al., 2009; Casola et al., 2006; Croker et al., 2004; Crouch et
287 al., 2007; de Boer et al., 2003; Dogan et al., 2009; Duber et al., 2009; Georgiades et al., 2002; Hobeika
288 et al., 2006; Kraus et al., 2004; Kwon et al., 2008; Moriyama et al., 2014; Robbiani et al., 2008;
289 Schweighoffer et al., 2013; Shinnakasu et al., 2016; Weber et al., 2019; Yasuda et al., 2013).

290

291 Here we used a systematic analysis of PC associated factors for which expression is increased during
292 PC differentiation (*Xbp1*, *Jchain*, *Scd1*, *Irf4*, and *Prdm1*) with the aim of identifying suitable candidates
293 for the generation of PC-specific tools. *Blimp1*, a critical transcription factor for the establishment of
294 the PC program, displayed an expression pattern unspecific to PCs. This was unsurprising given the
295 knowledge that *Blimp1* is expressed by other hematopoietic and non-hematopoietic cells (John and
296 Garrett-Sinha, 2009), including germ cells (Ohinata et al., 2005). Amongst the analyzed factors we
297 found that *Jchain* displayed the highest RNA expression level in PCs and had the most PC-specific
298 expression pattern (**Fig. 1D**). We considered *Jchain* to be the most suitable candidate for the generation
299 of PC-specific tools.

300

301 We searched among alleles generated by the EUCOMMTools consortium and identified a *Jchain*^{creERT2}
302 allele which through a comprehensive series of experiments we validated for specific genetic
303 manipulation of PCs. Briefly, *Jchain* was expressed in a very small subset of B cells (<2%, primarily
304 GC B cells; **Fig. 2F and G;** and **Fig. S1C**) and therefore preceded BLIMP1 and IRF4 expression (**Fig.
305 3C**). This data agrees with previous analysis of *in vitro* cultures of *Blimp1* deficient B cells in which it
306 was shown that the initiation of *Jchain* expression does not require BLIMP1 (Kallies et al., 2007). Thus
307 the identified population of cells *in vivo* marked by low GFP expression and high surface expression of
308 B220 (GFP^{low}B220^{hi}), where only ~7% of cells expressed BLIMP1 (**Fig. 3D** and **E**), likely contains PC

309 precursor cells and future analysis may provide information on the mechanisms underlying the very
310 first steps of PC differentiation.
311
312 *Jchain*^{creERT2} mediated genetic manipulation was only effective in PCs (**Fig. 4C** and **D**). In the
313 *Jchain*^{creERT2} allele GFP and cre^{ERT2} are linked by a self-cleaving 2A peptide which ensures a near
314 equitable co-expression of the proteins (Szymczak et al., 2004). As consequence, it is likely that
315 effectiveness of cre recombination correlates with level of cre^{ERT2} because PCs expressed the highest
316 level of *Jchain*, as suggested by the level of GFP expression (**Fig. 4C** and **D**). Of note, the *Jchain*^{creERT2}
317 allele analyzed in this work retained the puromycin selection cassette that is flanked by Rox
318 recombination sites (**Fig. 2A**). This knowledge should be taken in consideration in future experiments
319 involving compound mutant mice that make use of dre recombinase (Anastassiadis et al., 2009). On
320 occasion it has been observed that retention of the selection cassette reduces gene expression of the
321 targeted locus (Meyers et al., 1998; Nagy et al., 1998). As consequence inadvertent or intentional
322 removal of the puromycin selection cassette may potentiate increase creERT2 expression, including in
323 B cells, and as consequence reduce the PC specificity of *Jchain*^{creERT2} mediated genetic manipulation.
324 Lastly, in the *Jchain*^{creERT2} allele the expression of *Jchain* is interrupted by a GFP-2A-creERT2 cassette
325 and induction of cre-mediated recombination deletes *Jchain* exon 2 that is loxP-flanked. It was
326 previously shown that heterozygous deletion of *Jchain* displayed an intermediate phenotype to that of
327 knockout mice (Lycke et al., 1999). This knowledge must be taken into consideration when performing
328 *Jchain*^{creERT2} mediated genetic manipulation, including the need to use the *Jchain*^{creERT2} allele without
329 the targeted manipulation as control, and the utility of the *Jchain*^{creERT2} allele in homozygosity. Future
330 iterations of the *Jchain*^{creERT2} in which JCHAIN protein expression is preserved should be considered.
331
332 It is generally assumed that *Jchain* expression occurs in all PCs regardless of their isotypes (Castro and
333 Flajnik, 2014; Johansen et al., 2000; Mather et al., 1981). The characterization of the *Jchain*^{creERT2} allele
334 demonstrated at the single cell level that *Jchain* expression indeed occurs in PCs across
335 immunoglobulin isotypes (**Fig. 5**). However, our analysis did not support the concept that *Jchain* is
336 expressed by all PCs. The occurrence of *Jchain*$^{+}$ and *Jchain*^{neg} is of interest as it may provide insights

337 into PC development and should be a subject of further investigation in the future (Castro and Flajnik,
338 2014).
339
340 Using the *Jchain*^{creERT2} allele we performed inclusive genetic timestamping of PCs, independent of the
341 time at which cells were generated, cell cycle status, and localization (**Fig. 6**). We uncovered that the
342 numbers of total PCs and that of *Jchain*$^{+}$ PCs, which represent 70 to 90% of all PCs (**Fig. 6B** and **C**),
343 remained stable in spleen and bone marrow for at least 5 months (**Fig S2B** and **C**). Notably, within the
344 *Jchain*$^{+}$ PC population, cell decay was compensated by the emergence of new PCs (**Fig. 6B-G**),
345 supporting that PC turnover is homeostatically regulated. Homeostatic control of mature B cell numbers
346 is widely accepted (Crowley et al., 2009). In mature B cells the expression of a B cell receptor is crucial
347 for cell survival (Srinivasan et al., 2009); however, BAFF is the limited resource that defines the
348 boundaries of the biological "space" (Crowley et al., 2009; Srinivasan et al., 2009). On other hand, the
349 regulation of PC turnover remains unclear. PCs express the BCMA receptor that allows the sensing of
350 both BAFF and APRIL, and BCMA deficient mice have reduced PC numbers (O'Connor et al., 2004).
351 However, because BCMA is expressed in B cells committed to PC differentiation further studies are
352 required to disentangle formation and maintenance (Mackay et al., 2003). The *Jchain*^{creERT2} allele is
353 therefore ideally suited to tackle these questions. PC homeostatic regulation could also be the reflection
354 of a limited number of niches in a given organ which would then limit the number of PCs (Hofer et al.,
355 2006; Khodadadi et al., 2019; Lightman et al., 2019; Lindquist et al., 2019; Wilmore and Allman, 2017).
356 Knowledge on the underlying PC turnover mechanisms is important as these are directly related to long-
357 term protection from infection, vaccination and pathogenesis. The *Jchain*^{creERT2} allele is highly suited
358 to for these investigations as it allows genetic manipulation of PCs in vivo in their microenvironment,
359 and to retrieve live time-stamped PCs for downstream analysis.
360
361
362
363
364

Acknowledgments

We thank the members of the Immunity and Cancer laboratory (FCI, London) for critical discussions and review of the manuscript; the FCI BRF and Flow-cytometry platforms for expert advice and technical support.

This work was supported by The Francis Crick Institute which receives its core funding from Cancer Research UK (FC001057), the UK Medical Research Council (FC001057), the Wellcome Trust (FC001057), the CRUK accelerator award EDITOR, and an MRC career development award MR/J008060/1 to D.P.C.

The authors declare no competing financial interests.

Author contributions: Conceptualization, A.Q.X., R.R.B, D.P.C.; Methodology, A.Q.X., R.R.B, D.P.C.; Investigation, A.Q.X., R.R.B, D.P.C.; Resources, D.P.C.; Writing – Original Draft, A.Q.X., and D.P.C.; Supervision D.P.C.; Funding Acquisition, D.P.C.

393 **References**

394 Alugupalli, K.R., J.M. Leong, R.T. Woodland, M. Muramatsu, T. Honjo, and R.M. Gerstein. 2004.
395 B1b lymphocytes confer T cell-independent long-lasting immunity. *Immunity* 21:379-390.
396 Anastassiadis, K., J. Fu, C. Patsch, S. Hu, S. Weidlich, K. Duerschke, F. Buchholz, F. Edenhofer, and
397 A.F. Stewart. 2009. Dre recombinase, like Cre, is a highly efficient site-specific recombinase
398 in E. coli, mammalian cells and mice. *Dis Model Mech* 2:508-515.
399 Andersson, J., O. Sjoberg, and G. Moller. 1972. Induction of immunoglobulin and antibody synthesis
400 in vitro by lipopolysaccharides. *Eur J Immunol* 2:349-353.
401 Bonami, R.H., W.T. Wolfle, J.W. Thomas, and P.L. Kendall. 2014. NFATc2 (NFAT1) assists BCR-
402 mediated anergy in anti-insulin B cells. *Mol Immunol* 62:321-328.
403 Boross, P., C. Breukel, P.F. van Loo, J. van der Kaa, J.W. Claassens, H. Bujard, K. Schonig, and J.S.
404 Verbeek. 2009. Highly B lymphocyte-specific tamoxifen inducible transgene expression of
405 CreER T2 by using the LC-1 locus BAC vector. *Genesis* 47:729-735.
406 Brandtzaeg, P., and H. Prydz. 1984. Direct evidence for an integrated function of J chain and
407 secretory component in epithelial transport of immunoglobulins. *Nature* 311:71-73.
408 Calado, D.P., B. Zhang, L. Srinivasan, Y. Sasaki, J. Seagal, C. Unitt, S. Rodig, J. Kutok, A.
409 Tarakhovsky, M. Schmidt-Supprian, and K. Rajewsky. 2010. Constitutive canonical NF-
410 kappaB activation cooperates with disruption of BLIMP1 in the pathogenesis of activated B
411 cell-like diffuse large cell lymphoma. *Cancer Cell* 18:580-589.
412 Casola, S., G. Cattoretti, N. Uyttersprot, S.B. Koralov, J. Seagal, Z. Hao, A. Waisman, A. Egert, D.
413 Ghitza, and K. Rajewsky. 2006. Tracking germinal center B cells expressing germ-line
414 immunoglobulin gamma1 transcripts by conditional gene targeting. *Proc Natl Acad Sci U S A*
415 103:7396-7401.
416 Castro, C.D., and M.F. Flajnik. 2014. Putting J chain back on the map: how might its expression
417 define plasma cell development? *J Immunol* 193:3248-3255.
418 Croker, B.A., D. Metcalf, L. Robb, W. Wei, S. Mifsud, L. DiRago, L.A. Cluse, K.D. Sutherland, L.
419 Hartley, E. Williams, J.G. Zhang, D.J. Hilton, N.A. Nicola, W.S. Alexander, and A.W.
420 Roberts. 2004. SOCS3 is a critical physiological negative regulator of G-CSF signaling and
421 emergency granulopoiesis. *Immunity* 20:153-165.
422 Crouch, E.E., Z. Li, M. Takizawa, S. Fichtner-Feigl, P. Gourzi, C. Montano, L. Feigenbaum, P.
423 Wilson, S. Janz, F.N. Papavasiliou, and R. Casellas. 2007. Regulation of AID expression in
424 the immune response. *J Exp Med* 204:1145-1156.
425 Crowley, J.E., J.E. Stadanlick, J.C. Cambier, and M.P. Cancro. 2009. FcgammaRIIB signals inhibit
426 BLyS signaling and BCR-mediated BLyS receptor up-regulation. *Blood* 113:1464-1473.
427 de Boer, J., A. Williams, G. Skavdis, N. Harker, M. Coles, M. Tolaini, T. Norton, K. Williams, K.
428 Roderick, A.J. Potocnik, and D. Kioussis. 2003. Transgenic mice with hematopoietic and
429 lymphoid specific expression of Cre. *Eur J Immunol* 33:314-325.
430 Dogan, I., B. Bertocci, V. Vilmont, F. Delbos, J. Megret, S. Storck, C.A. Reynaud, and J.C. Weill.
431 2009. Multiple layers of B cell memory with different effector functions. *Nat Immunol*
432 10:1292-1299.
433 Duber, S., M. Hafner, M. Krey, S. Lienenklaus, B. Roy, E. Hobeika, M. Reth, T. Buch, A. Waisman,
434 K. Kretschmer, and S. Weiss. 2009. Induction of B-cell development in adult mice reveals the
435 ability of bone marrow to produce B-1a cells. *Blood* 114:4960-4967.
436 Feil, S., N. Valtcheva, and R. Feil. 2009. Inducible Cre mice. *Methods Mol Biol* 530:343-363.
437 Georgiades, P., S. Ogilvy, H. Duval, D.R. Licence, D.S. Charnock-Jones, S.K. Smith, and C.G. Print.
438 2002. VavCre transgenic mice: a tool for mutagenesis in hematopoietic and endothelial
439 lineages. *Genesis* 34:251-256.
440 Hargreaves, D.C., P.L. Hyman, T.T. Lu, V.N. Ngo, A. Bidgol, G. Suzuki, Y.R. Zou, D.R. Littman,
441 and J.G. Cyster. 2001. A coordinated change in chemokine responsiveness guides plasma cell
442 movements. *J Exp Med* 194:45-56.
443 Heng, T.S., M.W. Painter, and C. Immunological Genome Project. 2008. The Immunological Genome
444 Project: networks of gene expression in immune cells. *Nat Immunol* 9:1091-1094.
445 Ho, F., J.E. Lortan, I.C. MacLennan, and M. Khan. 1986. Distinct short-lived and long-lived
446 antibody-producing cell populations. *Eur J Immunol* 16:1297-1301.

447 Hobeika, E., S. Thiemann, B. Storch, H. Jumaa, P.J. Nielsen, R. Pelanda, and M. Reth. 2006. Testing
448 gene function early in the B cell lineage in mb1-cre mice. *Proc Natl Acad Sci U S A*
449 103:13789-13794.
450 Hofer, T., G. Muehlinghaus, K. Moser, T. Yoshida, E.M. H, K. Hebel, A. Hauser, B. Hoyer, O.L. E,
451 T. Dorner, R.A. Manz, F. Hiepe, and A. Radbruch. 2006. Adaptation of humoral memory.
452 *Immunol Rev* 211:295-302.
453 Johansen, F.E., R. Braathen, and P. Brandtzaeg. 2000. Role of J chain in secretory immunoglobulin
454 formation. *Scand J Immunol* 52:240-248.
455 John, S.A., and L.A. Garrett-Sinha. 2009. Blimp1: a conserved transcriptional repressor critical for
456 differentiation of many tissues. *Exp Cell Res* 315:1077-1084.
457 Kallies, A., J. Hasbold, K. Fairfax, C. Pridans, D. Emslie, B.S. McKenzie, A.M. Lew, L.M. Corcoran,
458 P.D. Hodgkin, D.M. Tarlinton, and S.L. Nutt. 2007. Initiation of plasma-cell differentiation is
459 independent of the transcription factor Blimp-1. *Immunity* 26:555-566.
460 Khodadadi, L., Q. Cheng, A. Radbruch, and F. Hiepe. 2019. The Maintenance of Memory Plasma
461 Cells. *Front Immunol* 10:721.
462 Klein, U., S. Casola, G. Cattoretti, Q. Shen, M. Lia, T. Mo, T. Ludwig, K. Rajewsky, and R. Dalla-
463 Favera. 2006. Transcription factor IRF4 controls plasma cell differentiation and class-switch
464 recombination. *Nat Immunol* 7:773-782.
465 Kraus, M., M.B. Alimzhanov, N. Rajewsky, and K. Rajewsky. 2004. Survival of resting mature B
466 lymphocytes depends on BCR signaling via the Igalpha/beta heterodimer. *Cell* 117:787-800.
467 Kwon, K., C. Hutter, Q. Sun, I. Bilic, C. Cobaleda, S. Malin, and M. Busslinger. 2008. Instructive
468 role of the transcription factor E2A in early B lymphopoiesis and germinal center B cell
469 development. *Immunity* 28:751-762.
470 Lemke, A., M. Kraft, K. Roth, R. Riedel, D. Lammerding, and A.E. Hauser. 2016. Long-lived plasma
471 cells are generated in mucosal immune responses and contribute to the bone marrow plasma
472 cell pool in mice. *Mucosal Immunol* 9:83-97.
473 Lightman, S.M., A. Utley, and K.P. Lee. 2019. Survival of Long-Lived Plasma Cells (LLPC): Piecing
474 Together the Puzzle. *Front Immunol* 10:965.
475 Lindquist, R.L., R.A. Niesner, and A.E. Hauser. 2019. In the Right Place, at the Right Time:
476 Spatiotemporal Conditions Determining Plasma Cell Survival and Function. *Front Immunol*
477 10:788.
478 Luche, H., O. Weber, T. Nageswara Rao, C. Blum, and H.J. Fehling. 2007. Faithful activation of an
479 extra-bright red fluorescent protein in "knock-in" Cre-reporter mice ideally suited for lineage
480 tracing studies. *Eur J Immunol* 37:43-53.
481 Lycke, N., L. Erlandsson, L. Ekman, K. Schon, and T. Leanderson. 1999. Lack of J chain inhibits the
482 transport of gut IgA and abrogates the development of intestinal antitoxic protection. *J*
483 *Immunol* 163:913-919.
484 Mackay, F., P. Schneider, P. Rennert, and J. Browning. 2003. BAFF AND APRIL: a tutorial on B cell
485 survival. *Annu Rev Immunol* 21:231-264.
486 Manz, R.A., M. Lohning, G. Cassese, A. Thiel, and A. Radbruch. 1998. Survival of long-lived plasma
487 cells is independent of antigen. *Int Immunol* 10:1703-1711.
488 Manz, R.A., A. Thiel, and A. Radbruch. 1997. Lifetime of plasma cells in the bone marrow. *Nature*
489 388:133-134.
490 Mather, E.L., F.W. Alt, A.L. Bothwell, D. Baltimore, and M.E. Koshland. 1981. Expression of J chain
491 RNA in cell lines representing different stages of B lymphocyte differentiation. *Cell* 23:369-
492 378.
493 Max, E.E., and S.J. Korsmeyer. 1985. Human J chain gene. Structure and expression in B lymphoid
494 cells. *J Exp Med* 161:832-849.
495 Meyers, E.N., M. Lewandoski, and G.R. Martin. 1998. An Fgf8 mutant allelic series generated by
496 Cre- and Flp-mediated recombination. *Nat Genet* 18:136-141.
497 Moriyama, S., N. Takahashi, J.A. Green, S. Hori, M. Kubo, J.G. Cyster, and T. Okada. 2014.
498 Sphingosine-1-phosphate receptor 2 is critical for follicular helper T cell retention in germinal
499 centers. *J Exp Med* 211:1297-1305.

500 Nagy, A., C. Moens, E. Ivanyi, J. Pawling, M. Gertsenstein, A.K. Hadjantonakis, M. Pirity, and J.
501 Rossant. 1998. Dissecting the role of N-myc in development using a single targeting vector to
502 generate a series of alleles. *Curr Biol* 8:661-664.
503 Nutt, S.L., P.D. Hodgkin, D.M. Tarlinton, and L.M. Corcoran. 2015. The generation of antibody-
504 secreting plasma cells. *Nat Rev Immunol* 15:160-171.
505 O'Connor, B.P., V.S. Raman, L.D. Erickson, W.J. Cook, L.K. Weaver, C. Ahonen, L.L. Lin, G.T.
506 Mantchev, R.J. Bram, and R.J. Noelle. 2004. BCMA is essential for the survival of long-lived
507 bone marrow plasma cells. *J Exp Med* 199:91-98.
508 Ohinata, Y., B. Payer, D. O'Carroll, K. Ancelin, Y. Ono, M. Sano, S.C. Barton, T. Obukhanych, M.
509 Nussenzweig, A. Tarakhovsky, M. Saitou, and M.A. Surani. 2005. Blimp1 is a critical
510 determinant of the germ cell lineage in mice. *Nature* 436:207-213.
511 Palumbo, A., and K. Anderson. 2011. Multiple myeloma. *N Engl J Med* 364:1046-1060.
512 Pracht, K., J. Meinzinger, P. Daum, S.R. Schulz, D. Reimer, M. Hauke, E. Roth, D. Mielenz, C.
513 Berek, J. Corte-Real, H.M. Jack, and W. Schuh. 2017. A new staining protocol for detection
514 of murine antibody-secreting plasma cell subsets by flow cytometry. *Eur J Immunol* 47:1389-
515 1392.
516 Rickert, R.C., J. Roes, and K. Rajewsky. 1997. B lymphocyte-specific, Cre-mediated mutagenesis in
517 mice. *Nucleic Acids Res* 25:1317-1318.
518 Rinkenberger, J.L., J.J. Wallin, K.W. Johnson, and M.E. Koshland. 1996. An interleukin-2 signal
519 relieves BSAP (Pax5)-mediated repression of the immunoglobulin J chain gene. *Immunity*
520 5:377-386.
521 Robbiani, D.F., A. Bothmer, E. Callen, B. Reina-San-Martin, Y. Dorsett, S. Difilippantonio, D.J.
522 Bolland, H.T. Chen, A.E. Corcoran, A. Nussenzweig, and M.C. Nussenzweig. 2008. AID is
523 required for the chromosomal breaks in c-myc that lead to c-myc/IgH translocations. *Cell*
524 135:1028-1038.
525 Schweighoffer, E., L. Vanes, J. Nys, D. Cantrell, S. McCleary, N. Smithers, and V.L. Tybulewicz.
526 2013. The BAFF receptor transduces survival signals by co-opting the B cell receptor
527 signaling pathway. *Immunity* 38:475-488.
528 Shaffer, A.L., M. Shapiro-Shelef, N.N. Iwakoshi, A.H. Lee, S.B. Qian, H. Zhao, X. Yu, L. Yang,
529 B.K. Tan, A. Rosenwald, E.M. Hurt, E. Petroulakis, N. Sonenberg, J.W. Yewdell, K. Calame,
530 L.H. Glimcher, and L.M. Staudt. 2004. XBP1, downstream of Blimp-1, expands the secretory
531 apparatus and other organelles, and increases protein synthesis in plasma cell differentiation.
532 *Immunity* 21:81-93.
533 Shapiro-Shelef, M., K.I. Lin, L.J. McHeyzer-Williams, J. Liao, M.G. McHeyzer-Williams, and K.
534 Calame. 2003. Blimp-1 is required for the formation of immunoglobulin secreting plasma
535 cells and pre-plasma memory B cells. *Immunity* 19:607-620.
536 Shinnakasu, R., T. Inoue, K. Kometani, S. Moriyama, Y. Adachi, M. Nakayama, Y. Takahashi, H.
537 Fukuyama, T. Okada, and T. Kurosaki. 2016. Regulated selection of germinal-center cells
538 into the memory B cell compartment. *Nat Immunol* 17:861-869.
539 Slifka, M.K., R. Antia, J.K. Whitmire, and R. Ahmed. 1998. Humoral immunity due to long-lived
540 plasma cells. *Immunity* 8:363-372.
541 Srinivasan, L., Y. Sasaki, D.P. Calado, B. Zhang, J.H. Paik, R.A. DePinho, J.L. Kutok, J.F. Kearney,
542 K.L. Otipoby, and K. Rajewsky. 2009. PI3 kinase signals BCR-dependent mature B cell
543 survival. *Cell* 139:573-586.
544 Sze, D.M., K.M. Toellner, C. Garcia de Vinuesa, D.R. Taylor, and I.C. MacLennan. 2000. Intrinsic
545 constraint on plasmablast growth and extrinsic limits of plasma cell survival. *J Exp Med*
546 192:813-821.
547 Szymczak, A.L., C.J. Workman, Y. Wang, K.M. Vignali, S. Dilioglou, E.F. Vanin, and D.A. Vignali.
548 2004. Correction of multi-gene deficiency in vivo using a single 'self-cleaving' 2A peptide-
549 based retroviral vector. *Nat Biotechnol* 22:589-594.
550 Weber, T., J. Seagal, W. Winkler, T. Wirtz, V.T. Chu, and K. Rajewsky. 2019. A novel allele for
551 inducible Cre expression in germinal center B cells. *Eur J Immunol* 49:192-194.
552 Wilmore, J.R., and D. Allman. 2017. Here, There, and Anywhere? Arguments for and against the
553 Physical Plasma Cell Survival Niche. *J Immunol* 199:839-845.

554 Yasuda, T., T. Wirtz, B. Zhang, T. Wunderlich, M. Schmidt-Supprian, T. Sommermann, and K.
555 Rajewsky. 2013. Studying Epstein-Barr virus pathologies and immune surveillance by
556 reconstructing EBV infection in mice. *Cold Spring Harb Symp Quant Biol* 78:259-263.
557
558
559
560
561
562
563
564
565
566
567
568
569
570
571
572
573
574
575
576
577
578
579
580
581
582
583

584 **Figure legends**

585 **Figure 1. *Jchain* transcripts are highly enriched in plasma cells.**

586 **(A)** Schematic of the network of factors associated with plasma cell differentiation. Upwards arrows
587 indicate increased expression compared to the precursor population. **(B-D)** Differential gene
588 expression analysis using RNA sequencing data (ImmGen, (Heng et al., 2008)). (B) Analysis of *Xbp1*
589 and *Irf4*, which encode for XBP1 and IRF4, respectively. (C) Analysis of *Sdc1* and *Prdm1*, which
590 encode for CD138 and BLIMP1, respectively. (D) Analysis for *Jchain* (*Igj*) that encodes for
591 JCHAIN. "x" indicates fold change. Expression Value Normalized by DESeq2.
592 http://rstats.immgen.org/Skyline/skyline.html.

593

594 **Figure 2. *Jchain* is expressed in a very small fraction of GC B cells and in most Plasma cells**.

595 **(A)** Schematic of *Jchain* targeted allele Wtsi MGI:5633773. Rectangular boxes indicate exons, and
596 exon number is on top; pink triangle indicates a FRT sequence; EGFPcre^{ERT2} cassette contains a splice
597 acceptor site (SA)-led EGFP-2A-creERT2 expression cassette followed by a poly-A tail inserted in the
598 intron between exons 1 and 2; white triangle indicates a ROX sequence; orange rectangle indicates a
599 promoter driven puromycin resistance cassette; green triangle indicates loxP sequence. **(B)** Schematic
600 of experimental procedure protocol. Mice carrying the *Jchain*^{creERT2} allele were immunized with sheep
601 red blood cells (SRBC) intravenously (i.v.) on day 0 and spleens of mice were analyzed at day 12 post-
602 immunization. **(C)** Gating strategy of populations by flow-cytometry according to the expression of
603 GFP and B220 in mice carrying the *Jchain*^{creERT2} allele and wild-type B6 mice for negative control of
604 GFP expression. (**D)** Gating strategy by flow-cytometry for plasma cells within the GFP^{hi}B220^{low}
605 population using CD138^{+} and CD138^{+}CXCR4^{+} markers. **(E)** Cumulative data for CD138^{+} and
606 CD138^{+}CXCR4^{+} plasma cells analyzed as in (D). Top: fraction of CD138^{+} plasma cells; Bottom:
607 fraction of CD138^{+}CXCR4^{+} plasma cells within the four populations defined by flow-cytometry
608 according to the expression of GFP and B220 in mice carrying the *Jchain*^{creERT2} allele. **(F)** Gating
609 strategy by flow-cytometry for total CD138^{+} and CD138^{+}CXCR4^{+} plasma cells within GFP^{low}B220^{hi}
610 population. The CD138^{neg} cell fraction within the GFP^{low}B220^{hi} population was analyzed for the CD19
611 B cell marker and stained for CD38 and FAS to determine germinal center (GC) B cells. **(G)** Cumulative

612 data for the frequency of GC B cells within the CD138^{neg}GFP^{low}B220^{hi} population. Each symbol (E, G)
613 represents an individual mouse; small horizontal lines indicate median, minimum and maximum values.
614 ***=p≤0.001, ****=p≤0.0001 (unpaired Student's *t*-test). Data are representative of three independent
615 experiments (E, G).
616
617 **Figure 3. *Jchain* expression correlates with that of IRF4 and BLIMP1**
618 **(A)** Schematic of experimental procedure protocol. Mice carrying the *Jchain*^{creERT2} allele were
619 immunized with sheep red blood cells (SRBC) intravenously (i.v.) on day 0 and spleens of mice were
620 analyzed at day 12 post-immunization. **(B)** Gating strategy of populations by flow-cytometry according
621 to the expression of GFP and B220 in mice carrying the *Jchain*^{creERT2} allele. Wild-type B6 mice for
622 negative control of GFP expression. **(C)** Gating strategy for IRF4 and BLIMP1 expression by flow-
623 cytometry within the GFP^{neg}B220^{neg} population. **(D)** Gating strategy for IRF4 and BLIMP1 expression
624 by flow-cytometry within GFP^{low}B220^{hi}, GFP^{int}B220^{int} and GFP^{hi}B220^{low} populations, defined as in (B).
625 **(E)** Cumulative data for the frequency of BLIMP1^{+}IRF4^{+} cells within the four populations defined as
626 in (B). Each symbol in (E) represents an individual mouse; small horizontal lines indicate median,
627 minimum and maximum values. ns=not significant, ***=p≤0.001, ****=p≤0.0001 (unpaired Student's
628 *t*-test). Data are representative of three independent experiments (E).
629
630 **Figure 4. *Jchain*^{creERT2} mediated genetic manipulation is effective only in plasma cells**.
631 **(A)** Schematic of experimental procedure protocol. Mice carrying the *Jchain*^{creERT2} and *R26*^{lslRFP} alleles
632 were immunized with sheep red blood cells (SRBC) intravenously (i.v.) on day 0 and spleens (top) and
633 bone marrow (bottom) of mice were analyzed at day 12 post-immunization. A group of mice received
634 tamoxifen treatment for four consecutive days from day 7 to day 10 after immunization. **(B)** Gating
635 strategy of populations by flow-cytometry in spleen (top) and bone marrow (bottom) according to the
636 expression of GFP and B220 in mice carrying the *Jchain*^{creERT2} allele. Wild-type B6 mice for negative
637 control of GFP expression. **(C)** Gating strategy for GFP and RFP expression by flow-cytometry in the
638 four populations defined as in (B). Top: spleen; bottom: bone marrow. **(D)** Cumulative data for the

639 frequency and number of $GFP^{+}RFP^{+}$ cells within $GFP^{neg}B220^{neg}$, $GFP^{low}B220^{hi}$, $GFP^{int}B220^{int}$ and
640 $GFP^{hi}B220^{low}$ populations, defined as in (B). Top: spleen; bottom: bone marrow. Each symbol (D)
641 represents an individual mouse; small horizontal lines indicate median, minimum and maximum values.
642 ns=not significant, *=p≤0.05, **=p≤0.01, ***=p≤0.001, ****=p≤0.0001 (unpaired Student's *t*-test).
643 Data are representative of three independent experiments (D).
644
645 **Figure 5. Genetic manipulation using *Jchain*^{creERT2} occurs across immunoglobulin isotypes**.
646 **(A)** Schematic of experimental procedure protocol. Mice carrying the *Jchain*^{creERT2} and *R26*^{lslRFP} alleles
647 were immunized with sheep red blood cells (SRBC) intravenously (i.v.) on day 0 and spleens,
648 mesenteric lymph nodes (mLN), peyer's patches, and bone marrows of mice were analyzed at day 12
649 post-immunization. Mice received tamoxifen treatment for four consecutive days from day 7 to day 10
650 after immunization. **(B)** Gating strategy by flow-cytometry for intracellular and extracellular expression
651 of IgG1, IgM and IgA within total $B220^{low}CD138^{+}$ plasma cells. Analysis in the spleen is provided as
652 example. **(C)** Gating strategy by flow-cytometry for intracellular and extracellular expression of IgG1,
653 IgM and IgA within $B220^{low}CD138^{+}GFP^{+}$ (RFP^{+} and RFP^{neg}) plasma cells. Analysis in the spleen is
654 provided as example. **(D)** Gating strategy by flow-cytometry for intracellular and extracellular
655 expression of IgG1, IgM and IgA within $B220^{low}CD138^{+}GFP^{+}RFP^{+}$ plasma cells. Analysis in the spleen
656 is provided as example. **(E)** Cumulative data for the fractions of IgA, IgM or IgG1 expressing cells
657 within total plasma cells (PC) (black, $B220^{low}CD138^{+}$), GFP^{+} (RFP^{+} and RFP^{neg}) plasma cells (green,
658 $B220^{low}CD138^{+}GFP^{+}$), and $GFP^{+}RFP^{+}$ plasma cells (orange, $B220^{low}CD138^{+}GFP^{+}RFP^{+}$) at 15 weeks
659 of age. **(F)** Cumulative data for the fractions of IgA, IgM or IgG1 expressing cells within total plasma
660 cells (PC) (black, $B220^{low}CD138^{+}$), GFP^{+} (RFP^{+} and RFP^{neg}) plasma cells (green,
661 $B220^{low}CD138^{+}GFP^{+}$), and $GFP^{+}RFP^{+}$ plasma cells (orange, $B220^{low}CD138^{+}GFP^{+}RFP^{+}$) at 30 weeks
662 of age. Each symbol (E, F) represents an individual mouse; small horizontal lines indicate median,
663 minimum and maximum values. ns=not significant, *=p≤0.05 (2way ANOVA). Data are representative
664 of three independent experiments (E, F).
665

666 **Figure 6. Inclusive analysis of plasma cell dynamics reveals homeostatic population turnover.**
667 **(A)** Schematic of experimental procedure protocol. Mice carrying the *Jchain*^{creERT2} and *R26*^{lslRFP} alleles
668 were immunized twice with sheep red blood cells (SRBC) intravenously (i.v.) on day 0 and day 21.
669 Mice received tamoxifen treatment for five consecutive days from day 51 to 55 after the first
670 immunization. Spleens and bone marrow of mice were analyzed at the five-day, two-month and five-
671 month timepoints after the last tamoxifen administration. **(B)** Cumulative data for the absolute cell
672 numbers of total PCs, of GFP$^+$ cells (RFP$^+$ and RFP^{neg}, i.e. *Jchain*$^+$), GFP$^+$RFP$^+$ cells (i.e. *Jchain*$^+$ cre
673 recombined), and GFP$^+$RFP^{neg} cells (i.e. *Jchain*$^+$ not cre recombined) in the spleen. **(C)** Cumulative data
674 for the absolute cell numbers of total PCs, of GFP$^+$ cells (RFP$^+$ and RFP^{neg}, i.e. *Jchain*$^+$), GFP$^+$RFP$^+$
675 cells (i.e. *Jchain*$^+$ cre recombined), and GFP$^+$RFP^{neg} cells (i.e. *Jchain*$^+$ not cre recombined) in the bone
676 marrow. **(D)** Graphical representation of half-life ($t_{1/2}$) of GFP$^+$RFP$^+$CD138$^+$CXCR4$^+$ plasma cells in
677 the spleen using the data presented in (B). Graphing of best-fit curve was performed using the GraphPad
678 Prism 8 software. **(E)** Graphical representation of half-life ($t_{1/2}$) of GFP$^+$RFP$^+$CD138$^+$CXCR4$^+$ plasma
679 cells in the bone marrow using the data presented in (C). Graphing of best-fit curve was performed
680 using the GraphPad Prism 8 software. **(F)** Graphical representation of half-life ($t_{1/2}$) of
681 GFP$^+$RFP^{neg}CD138$^+$CXCR4$^+$ plasma cells in the spleen using the data presented in (B). Graphing of
682 best-fit curve was performed using the GraphPad Prism 8 software. **(G)** Graphical representation of
683 half-life ($t_{1/2}$) of GFP$^+$RFP^{neg}CD138$^+$CXCR4$^+$ plasma cells in the bone marrow using the data presented
684 in (C). Graphing of best-fit curve was performed using the GraphPad Prism 8 software. Each symbol
685 (B-G) represents an individual mouse; small horizontal lines indicate median, minimum and maximum
686 values. ns=not significant, *=p≤0.05 **=p≤0.01, ***=p≤0.001, ****=p≤0.0001 (unpaired Student's *t*-
687 test). Data are representative of three independent experiments (B, C).
688
689 **Supplemental Figure Legends**
690 **Figure S1. *Jchain* expression in multiple stages of B cell development and other cell lineages**
691 **(A)** Gating strategy by flow-cytometry for the B cell lineage in the spleen. Mice carrying the
692 *Jchain*^{creERT2} and *R26*^{lslRFP} alleles were immunized with sheep red blood cells (SRBC) intravenously
693 (i.v.) at day 0 and spleens were analyzed at day 12. Mice did not receive tamoxifen treatment. Cells

694 were pre-gated on live singlets and for the expression of CD138 and CXCR4 markers. CD138^{+}CXCR4^{+}
695 cells were defined as plasma cells (PC). Non-PCs positive for the CD19 and B220 markers were defined
696 as B2 cells, whereas those cells displaying a CD19^{+}B220^{low} were defined as B1 cells. B1 cells were
697 further characterized as B1a (CD5^{hi}CD23^{neg}) and B1b (CD5^{low}CD23^{neg}) cells. B2 cells were further
698 delineated into marginal zone (MZ) B cells (CD21^{hi}CD23^{int}), T1 B cells (CD21^{low}CD23^{low}), T2 B cells
699 (CD21^{int}IgM^{hi}CD23^{hi}) and Follicular B cells (Fo, CD21^{int}IgM^{int}CD23^{hi}. Non MZ or T1 cells were gated
700 for germinal center (GC) B cells (CD38^{low}FAS^{high}) and these were further delineated into dark zone GC
701 B cells (CXCR4^{high}CD86^{low}) and light zone GC B cells (CXCR4^{low}CD86^{high}). (Bonami et al., 2014) **(B)**
702 Cumulative data for fractions of GFP^{+}RFP^{neg} and GFP^{+}RFP^{+} cells within the B cell lineage in the spleen.
703 Analyzed as in (A). **(C)** Cumulative data for fractions of GFP^{+}RFP^{neg} cells and GFP^{+}RFP^{+} cells in
704 additional B cell lineage and non-B cell lineage populations in the spleen. Analyzed as in (A). **(D)**
705 Gating strategy by flow-cytometry for the B cell lineage in the bone marrow. Mice carrying the
706 *Jchain*^{creERT2} and *R26*^{lslRFP} alleles were immunized with sheep red blood cells (SRBC) intravenously
707 (i.v.) at day 0 and spleens were analyzed at day 12. Mice did not receive tamoxifen treatment. Cells
708 were pre-gated on live singlets and gated for CD138 and B220 expression. CD138^{+}B220^{low} cells were
709 defined as plasma cells (PCs) Non-PCs positive for the CD19 and B220 markers were further examined
710 and further delineated to immature B cells (IgM^{+}CD43^{neg}), Pre-B cells (fraction D; IgM^{neg}CD43^{neg}) and
711 Pro-B cells (IgM^{neg}CD43^{+}). Pro B cells were further sub-divided into Hardy fraction A (BP1^{neg}CD24^{neg}),
712 fraction B (BP1^{neg}CD24^{+}), fraction C (BP1^{+}CD24^{neg}) and fraction C' (BP1^{+}CD24^{+}). **(E)** Cumulative
713 data for fractions of GFP^{+}RFP^{neg} cells and GFP^{+}RFP^{+} cells in the B cell lineage and in plasma cells in
714 the bone marrow. Analyzed as in (D). Each symbol (B, C, E) represents an individual mouse; small
715 horizontal lines indicate median, minimum and maximum values. Data are representative of three
716 independent experiments (B, C, E).
717
718 **Figure S2. *Jchain*^{creERT2} mediated genetic manipulation in vitro**.
719 (**A**) Gating strategy by flow-cytometry for GFP and RFP expression within CD19^{+}B220^{+} B cells and
720 B220^{low}CD138^{+} plasmablasts. Splenic B cells from unmanipulated mice carrying the *Jchain*^{creERT2} and
721 *R26*^{lslRFP} alleles were enriched using CD43 negative depletion (MACS) and culture *in vitro* in the

722 presence of LPS and 4-hydroxytamoxifen (4-OH-TAM). Cells were analyzed 48h, 72h, and 96h time-
723 points for GFP and RFP expression by flow-cytometry. Data from 96h analysis of a B cell culture with
724 LPS and 1μM 4-OH-TAM is shown as example. (**B**) Cumulative data for fractions of $GFP^{neg}RFP^{neg}$,
725 $GFP^{+}RFP^{neg}$, $GFP^{+}RFP^{+}$ cells within B cells. Analyzed as in (A). (**C**) Cumulative data for fractions of
726 $GFP^{neg}RFP^{neg}$, $GFP^{+}RFP^{neg}$, $GFP^{+}RFP^{+}$ cells within plasmablasts. Analyzed as in (A).
727
728
729
730
731
732
733
734
735
736
737
738
739
740
741
742
743
744
745
746
747
748
749

750 **Materials and Methods**

751 **Mice:** The *Jchain*^{creERT2} allele was purchased from EMMA in agreement with the Wellcome Trust
752 Sanger Institute (Jchain targeted allele Wtsi MGI:5633773, genebank https://www.i-
753 dcc.org/imits/targ_rep/alleles/43805/escell-clone-genbank-file) and mice were rederived at the The
754 Francis Crick Institute. The allele contains a splice acceptor site (SA), an *EGFP-2A-creERT2*
755 expression cassette and a poly-A tail in the intron between exons 1 and 2 under the *Jchain* promoter. In
756 addition, exon 2 is loxP-flanked and the allele also contains a Rox-flanked puromycin resistance
757 cassette. These mice were crossed to carry a *Rosa26*^{lslRFP} cre recombination reporter allele (*R26*$^{lsl.RFP}$)
758 allele that expresses a non-toxic tandem-dimer red fluorescent protein upon cre-mediated deletion of a
759 floxed STOP cassette (Luche et al., 2007). Mice were maintained on the C57BL/6 background and bred
760 at The Francis Crick Institute biological resources facility under specific pathogen-free conditions.
761 Animal experiments were carried out in accordance with national and institutional guidelines for animal
762 care and were approved by The Francis Crick Institute biological resources facility strategic oversight
763 committee (incorporating the Animal Welfare and Ethical Review Body) and by the Home Office, UK.
764 All animal care and procedures followed guidelines of the UK Home Office according to the Animals
765 (Scientific Procedures) Act 1986 and were approved by Biological Research Facility at the Francis
766 Crick Institute. The age of mice ranged between 15-30 weeks as specified.

767

768 **Immunization and *in vivo* induction of cre activity**: Mice were injected intravenously with 1 x 10^9
769 sheep red blood cells (SRBCs, TCS Biosciences Ltd) in PBS. For the induction of cre activity, 4mg
770 tamoxifen (SIGMA T5648) dissolved in sunflower seed oil were administered by oral gavage to mice
771 once per day for multiple days depending on experimental design.

772

773 ***In vitro* B cell culture and induction cre activity**: Splenic cells were harvested and B cells were
774 isolated using CD43 (Ly-48) MicroBeads, mouse (Miltenyi Biotec). The purity of B cells was
775 determined by flow-cytometry (>95%). B cells were cultured in 96-well round-bottom plates (Falcon)
776 in B cell media in B cell media (DMEM high glucose/Glutamax from ThermoFisher Scientific
777 supplemented with 10% fetal bovine serum F7524 from Sigma, 100 U/mL Penicillin and 100 µg/mL

778 Streptomycin from Life Technologies, 10 mM HEPES Buffer Solution from Life Technologies, 100
779 μM MEM Non-essential Amino Acids from ThermoFisher Scientific, 1 mM sodium pyruvate from Life
780 Technologies and 50 uM β-mercaptoethanol from Sigma) at 1 million/mL concentration (200,000
781 cells/well) with 10ug/mL LPS and varied concentrations of (Z) 4-hydroxytamoxifen (Sigma-Aldrich).
782 Analysis was performed by flow-cytometry at 48, 72 or 96 hours of culture.
783
784 **Antibodies:** Rat Anti-Mouse Blimp-1, Clone 6D3 (BD Biosciences); Rat Anti-Mouse CD16/CD32,
785 Clone 2.4G2 (BD Biosciences); Rat Anti-Mouse CD19, Clone 1D3 (BD Biosciences); Rat Anti-Mouse
786 CD23, Clone B3B4 (BD Biosciences); Rat Anti-Mouse CD38, Clone 90 (BD Biosciences); Hamster
787 Anti-Mouse CD95, Clone Jo2 (BD Biosciences); Rat Anti-Mouse IgG1, Clone A85-1 (BD
788 Biosciences); Rat Anti-Mouse CD138, Clone 281-2 (BD Biosciences); Rat Anti-Mouse CD45R/B220,
789 Clone RA3-6B2 (BioLegend); Hamster Anti-Mouse CD11c, Clone N418 (BioLegend); Rat Anti-
790 Mouse CD19, Clone 6D5 (BioLegend); Rat Anti-Mouse CD21/35, Clone 7E9 (BioLegend); Rat Anti-
791 Mouse CD43, Clone 1B11 (BioLegend); Rat Anti-Mouse CD86, Clone GL1 (BioLegend); Rat Anti-
792 Mouse BP1, Clone 6C3 (eBioscience); Rat Anti-Mouse CD5, Clone 53-7.3 (eBioscience); Rat Anti-
793 Mouse CXCR4, Clone 2B11 (eBioscience); Rat Anti-Mouse IgA, Clone 11-44-2 (eBioscience); Rat
794 Anti-Mouse IgM, Clone II/41 (eBioscience); Rat Anti-mouse IRF4, Clone 3E4 (eBioscience).
795
796 **Flow cytometry**: Single cell suspensions were stained with antibodies. We used Zombie NIR Fixable
797 Viability Kit (BioLegend) for live/dead discrimination. For intracellular staining we fixed cells using
798 the BD CytoFix/Cytoperm (BD Biosciences) kit as per manufacturer instructions. Samples were
799 acquired on a BD LSRFortessa analyser using FACSDiva software (BD) and analysed on FlowJo
800 software.
801
802 **Quantification and statistical analysis:** Data were analyzed with unpaired two-tailed Student's t test
803 or 2way ANOVA; a p-value of 0.05 or less was considered significant. Prism (v7 and v8, GraphPad)
804 was used for statistical analysis. A single asterisk (*) in the graphs of figures represents a p-value ≤0.05,
805 double asterisks (**) a p-value ≤0.01, triple asterisks (***) a p-value ≤0.001, quadruple asterisks (****) a

806 p-value ≤0.0001, and "ns" stands for not statistically significant, i.e., a p-value >0.05.

807

808 **Online supplemental material:** Figure S1 displays the analysis of *Jchain* expression across cell
809 lineages in the spleen and bone marrow. These data also demonstrate that *Jchain*^{creERT2} mediated genetic
810 manipulation does not occur in the absence of tamoxifen treatment. Figure S2 shows experiments using
811 a classical LPS-induced B to plasmablast differentiation and the occurrence of *Jchain*^{creERT2} mediated
812 genetic manipulation upon addition of increasing concentrations of 4-hydroxytamoxifen (4-OH-TAM).

813

Figure 1.

Jchain transcripts are highly enriched in plasma cells

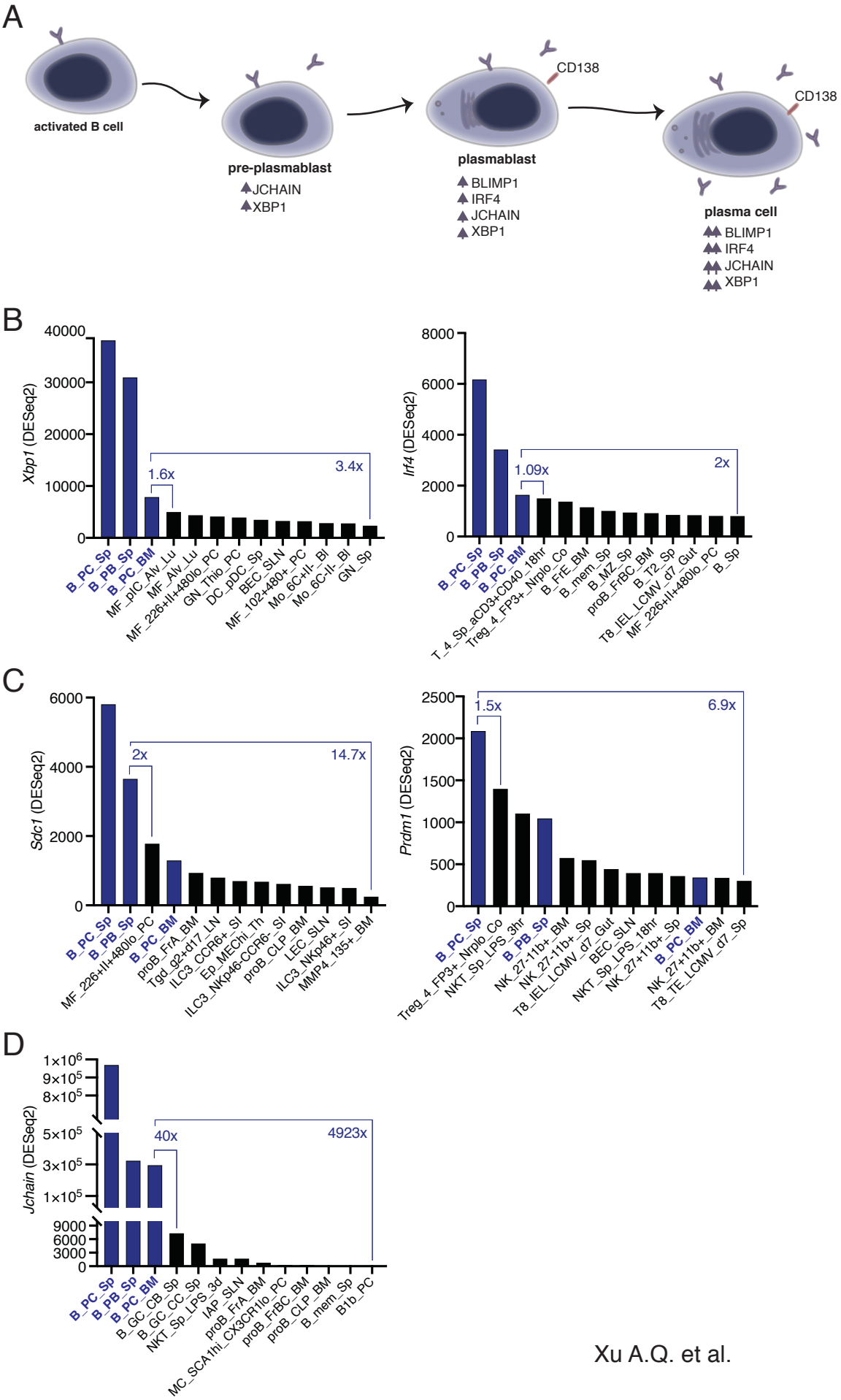

Xu A.Q. et al.

Figure 2.

Jchain is expressed in a very small fraction of GC B cells and in most plasma cells

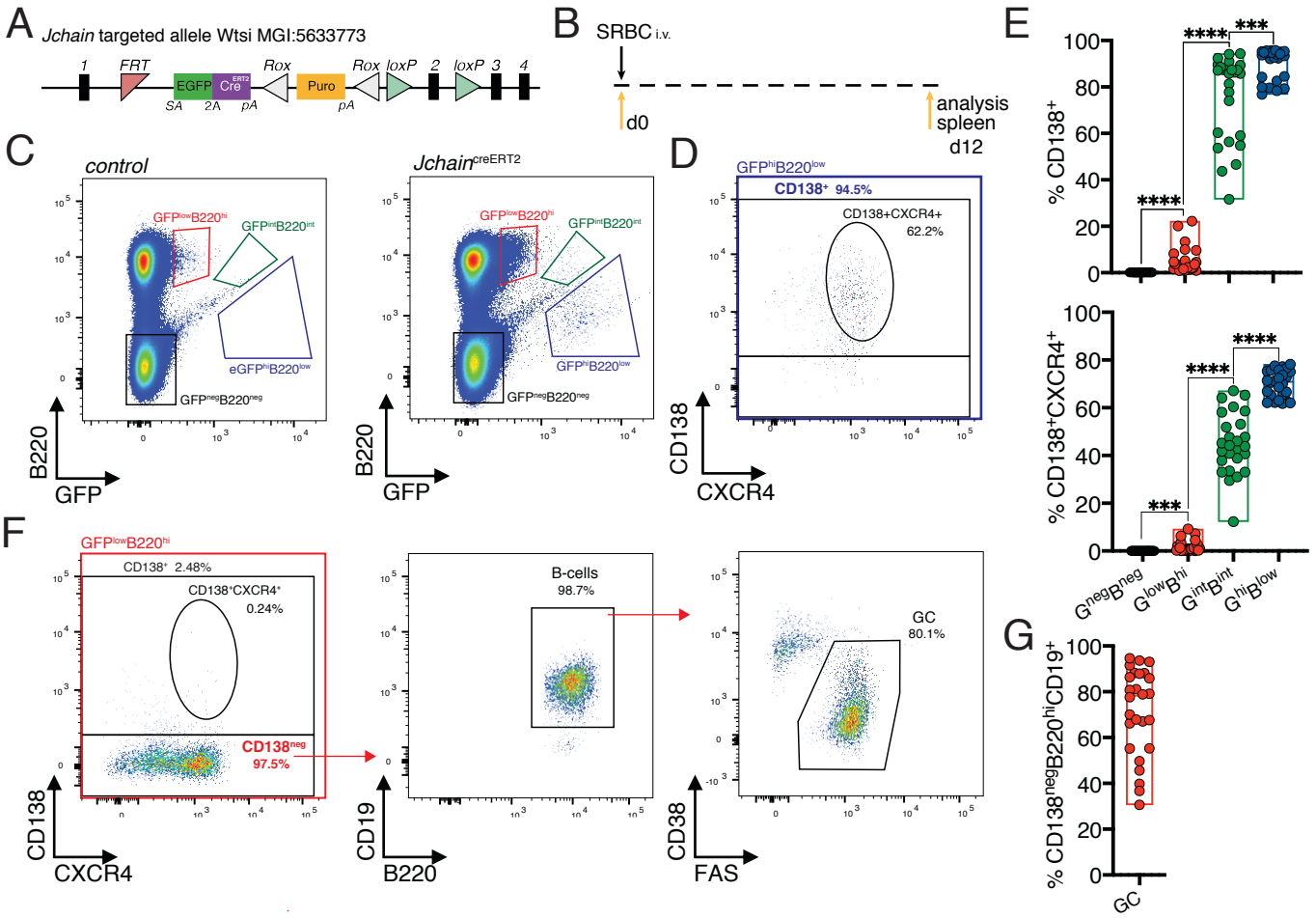

Xu A.Q. et al.

Figure 3.

Jchain expression correlates with that of IRF4 and BLIMP1

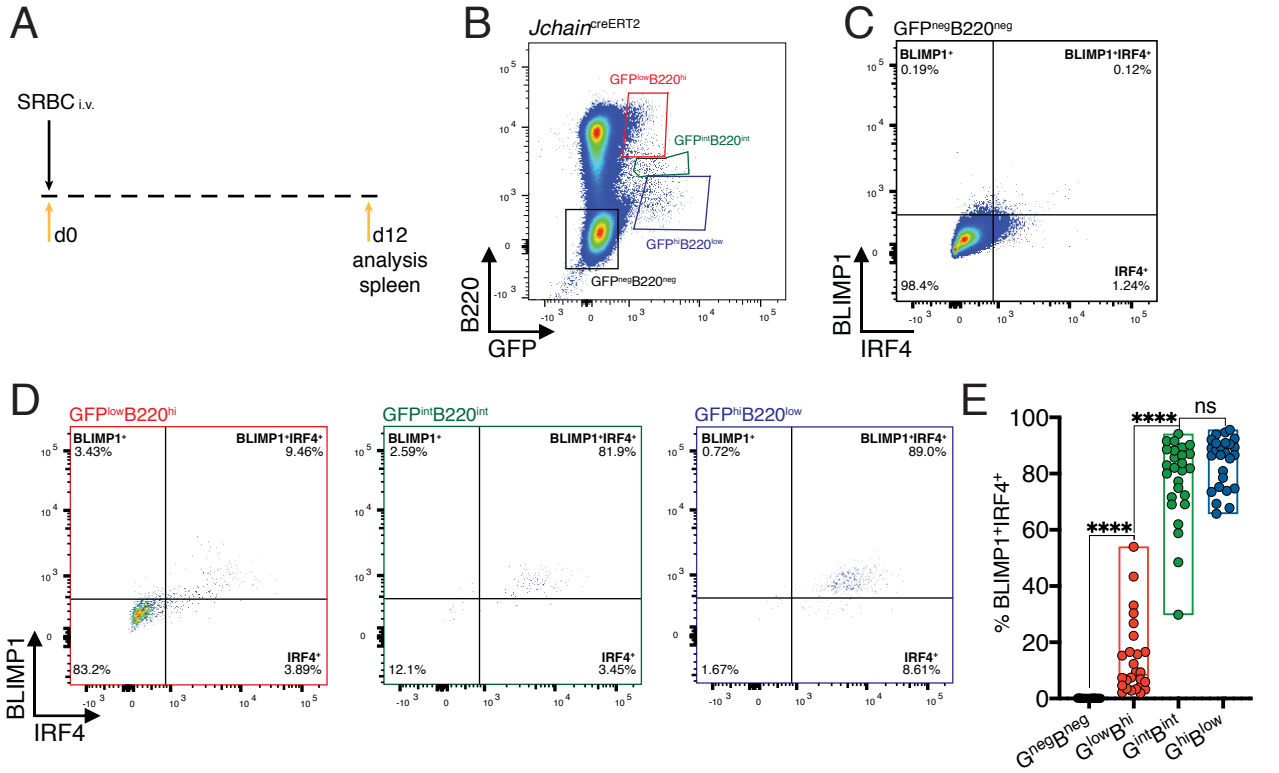

Xu A.Q. et al.

Figure 4.

Jchain^{creERT2} mediated genetic manipulation is effective only in plasma cells

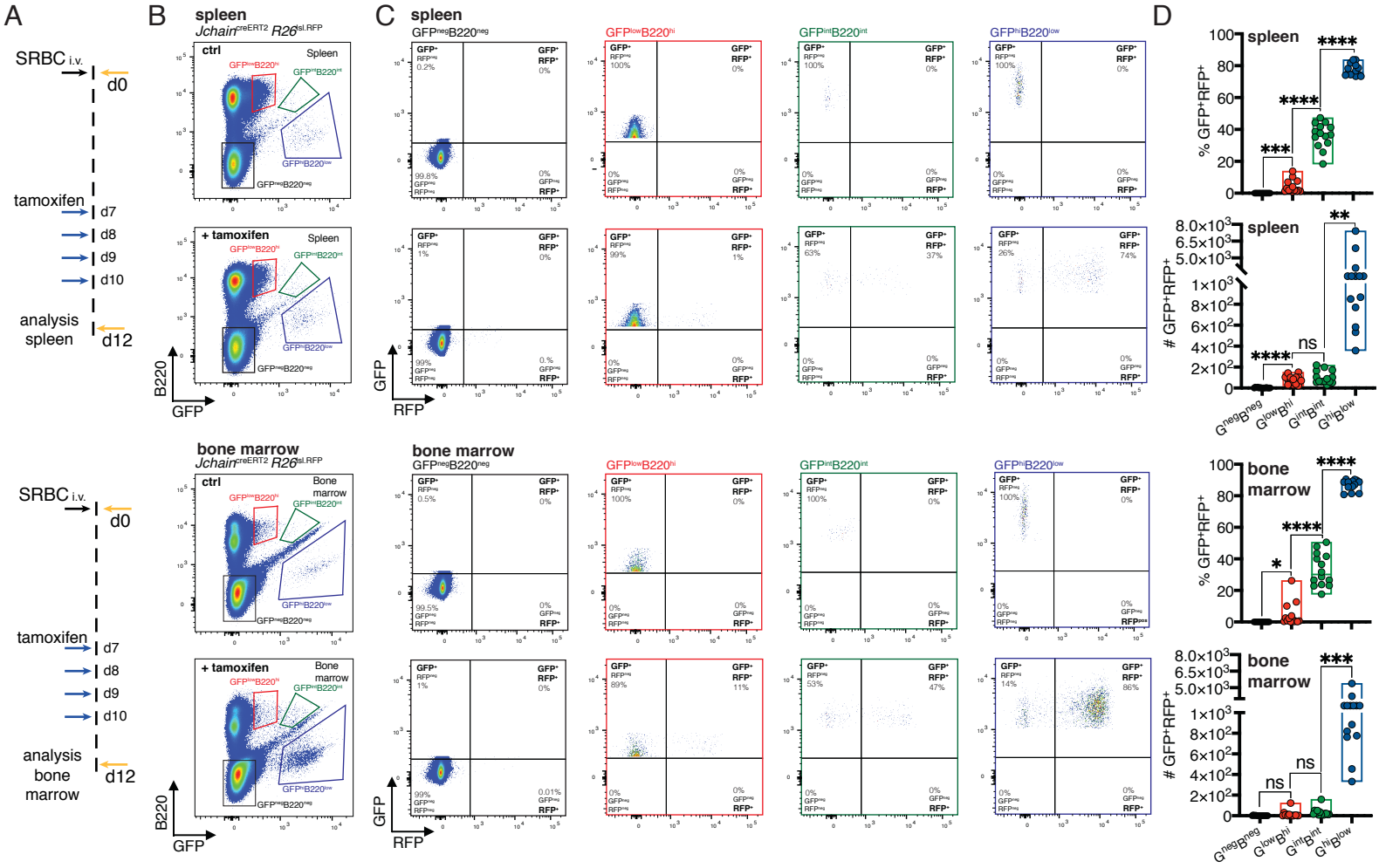

Figure 5.

Genetic manipulation using *Jchain*^{creERT2} occurs across immunoglobulin isotypes

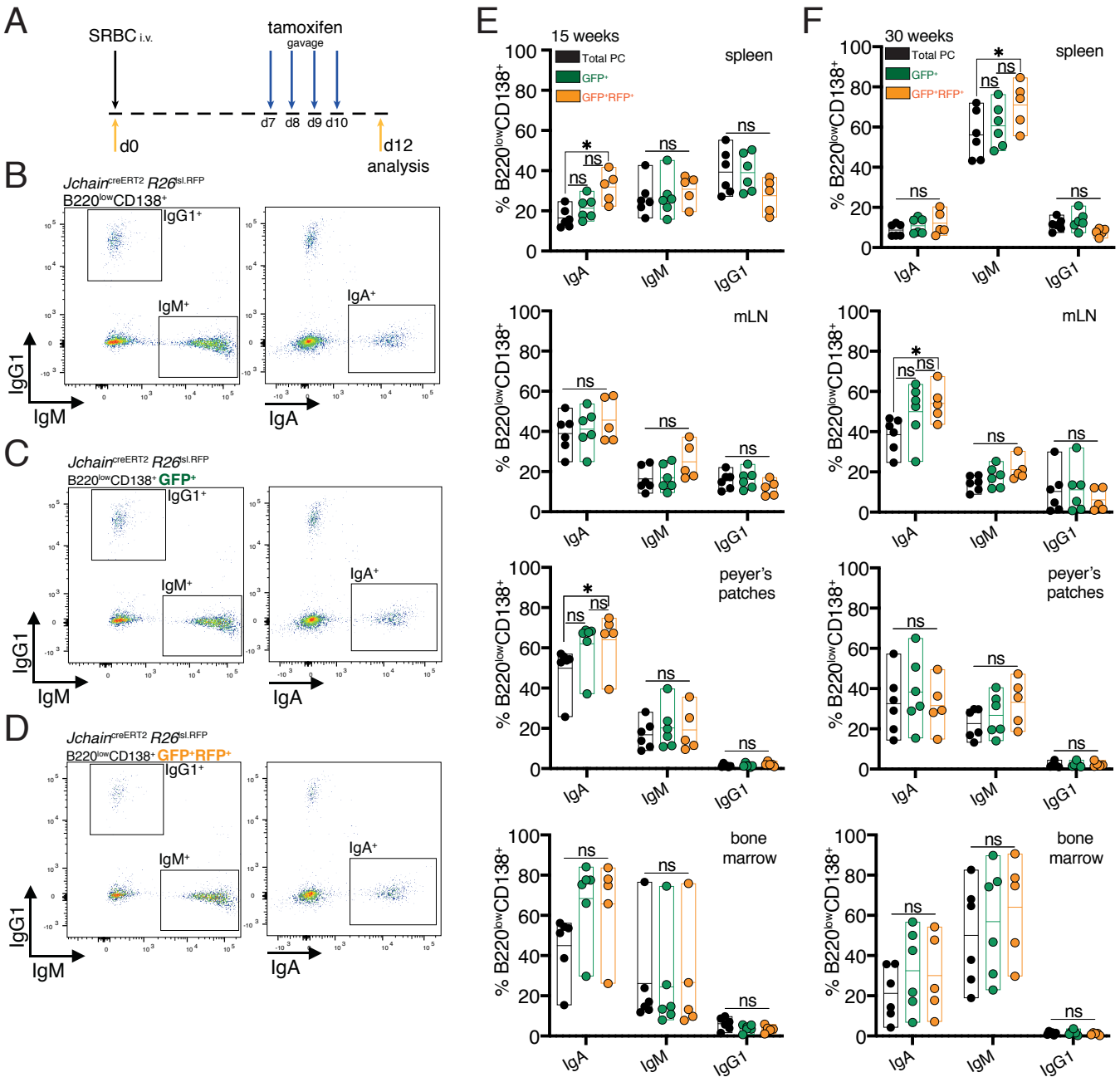

Xu A.Q. et al.

Figure 6.

Inclusive analysis of plasma cell dynamics reveals homeostatic population turnover

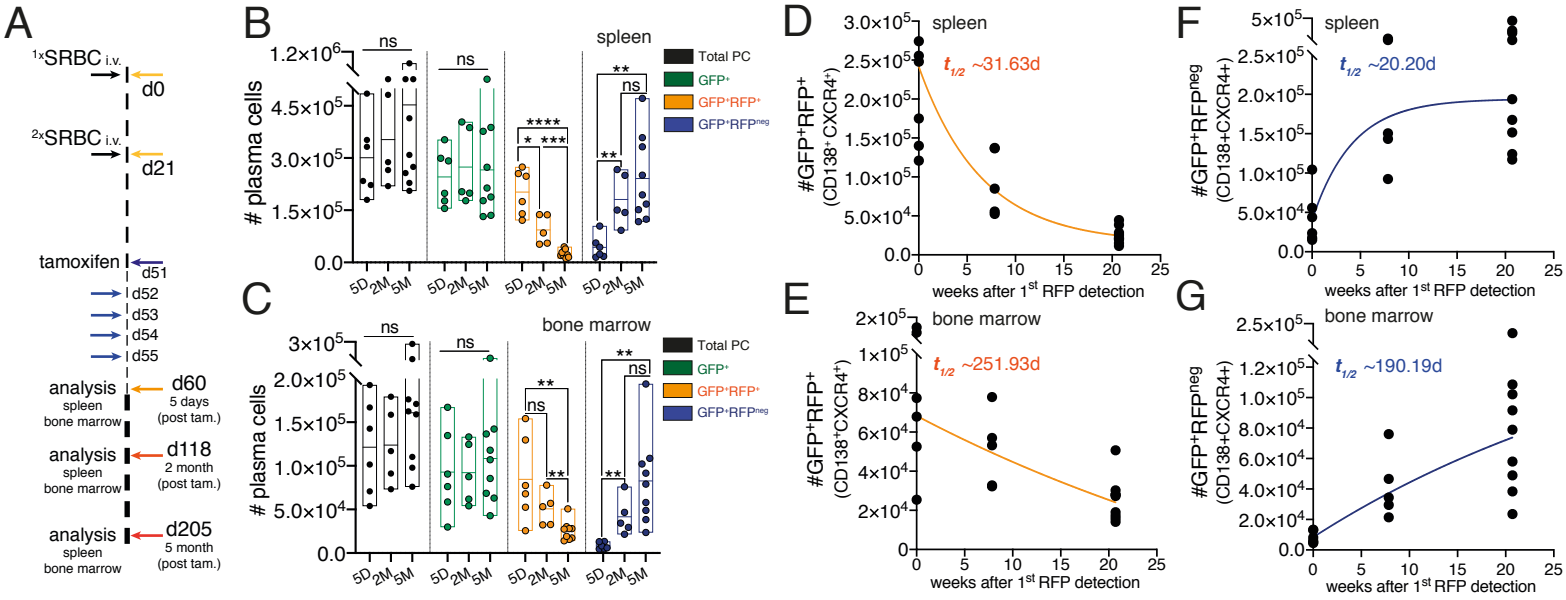

Xu A.Q. et al.

Figure S1.

Jchain expression in multiple stages of B cell development and other cell lineages

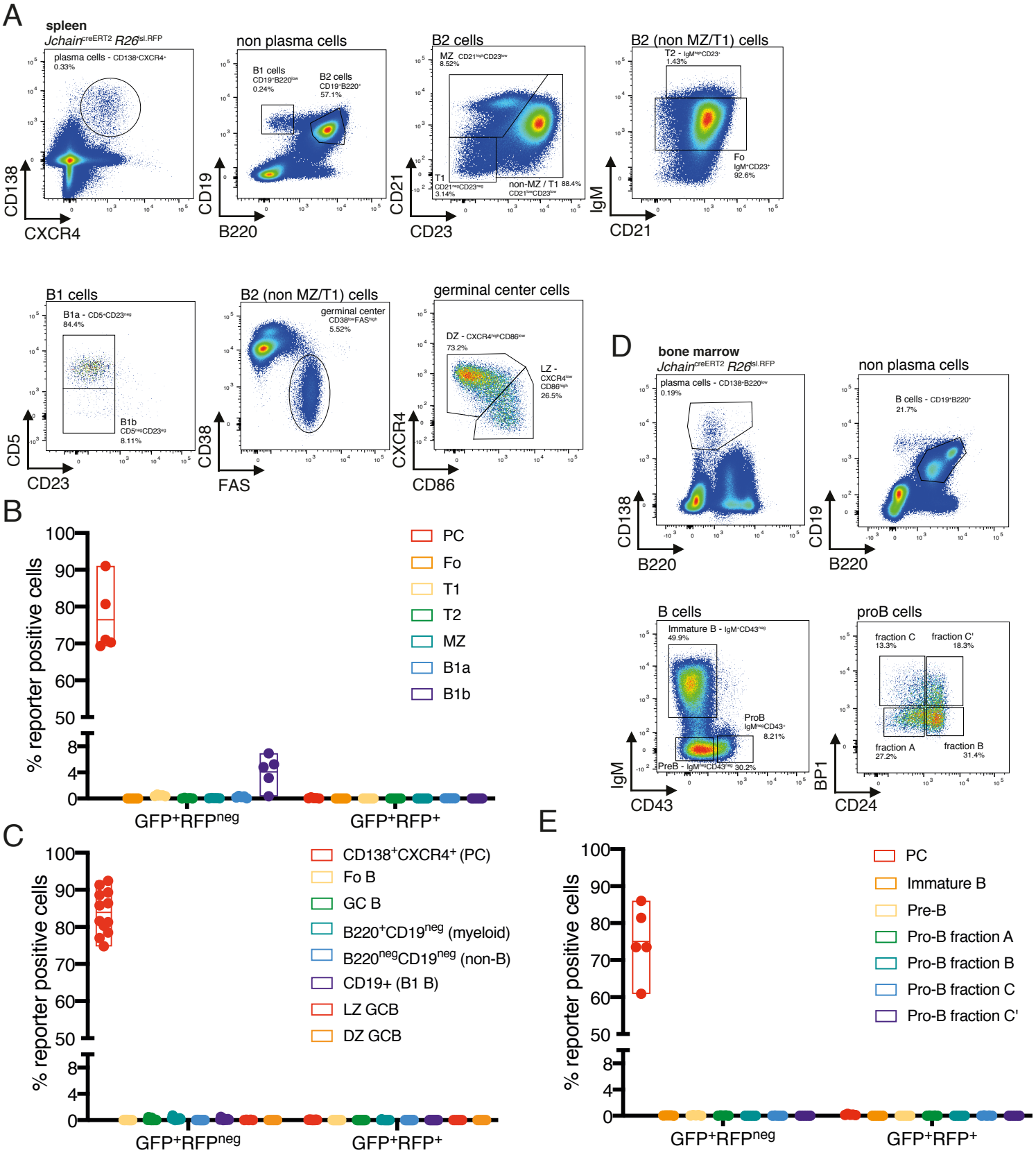

Xu A.Q. et al.

Figure S2.

Jchain^{creERT2} mediated genetic manipulation *in vitro*

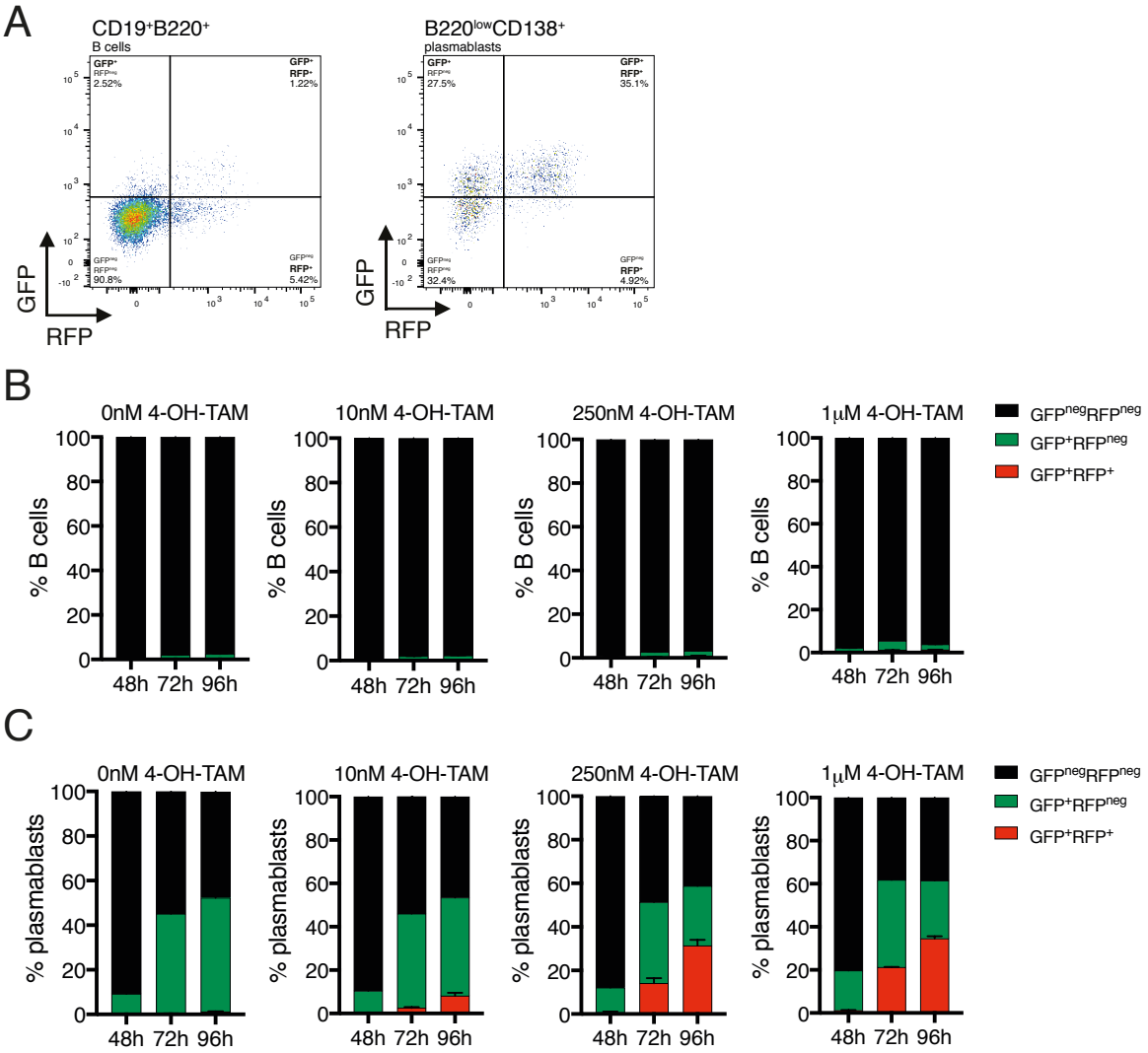

Xu A.Q. et al.